

Water-Fat MR Imaging for Assessing Changes in Bone Marrow Composition Due to Radiation and Chemotherapy in Gynecologic Cancer Patients

Patrick J Bolan¹, Luke Arentsen², Thanasak Sueblinvong³, Yan Zhang⁴, Steen Moeller¹, Jori Carter³, Levi S Downs³, Rahel Ghebre³, Douglas Yee^{4,5}, Jerry Froelich¹, and Susanta K Hui^{4,6}

¹Radiology, University of Minnesota, Minneapolis, MN, United States, ²Medical Physics, University of Minnesota, Minneapolis, Minnesota, United States, ³Obstetrics and Gynecology, University of Minnesota, Minneapolis, MN, United States, ⁴Masonic Cancer Center, University of Minnesota, Minneapolis, Minnesota, United States, ⁵Department of Medicine, University of Minnesota, Minneapolis, Minnesota, United States, ⁶Therapeutic Radiology, University of Minnesota, Minneapolis, Minnesota, United States

Introduction: Damage to bone marrow is caused by the common cancer therapies of radiation and chemotherapy. Both chemotherapy and radiation treatment can attenuate the production of red marrow and increase the production of fatty yellow marrow, thus leading to increased fat fractions. This marrow composition change is associated with reduced hematopoietic capacity and may contribute to bone mineral loss and increased fracture risk in cancer patients. The fat content of marrow is commonly visualized qualitatively using T1-weighted MRI, but has been studied quantitatively using MRS (1-4) and, to a lesser extent, 2D water-fat MRI techniques (5-7).

Purpose: To assess the feasibility of acquiring high-resolution, 3D signal fat fraction maps across multiple marrow regions and determine if they are sensitive to radiation- and chemotherapy-induced marrow composition changes.

Methods: Thirteen women with gynecologic malignancies who were to receive radiation and/or chemotherapy were recruited for this IRB-approved study. Subjects were imaged on a 3T MR scanner at baseline (after surgery but before radiation or chemotherapy), 6 months, and 12 months after treatment. Subjects were imaged in the supine position using body matrix and spine array coils. Water-fat source images were acquired using a 3D gradient echo (Siemens' f13d_vibe), TR=9 ms, flip angle=10°, matrix 320x320, square field of view 300-370 mm (typ. 350mm), slice thickness 2.45 mm, 176 axial slices (interpolated on the scanner to 288 1.5 mm slices), readout bandwidth 600 Hz/pixel, partial Fourier 6/8 in both phase encode directions, and GRAPPA acceleration R=2 (anterior-posterior) and R=3 (head-foot) with 24 integrated reference lines in each dimension, giving a total acceleration of R=6 and acquisition time of 57 s. Three consecutive images were acquired with TE=2, 3, and 4 ms, giving a total water-fat acquisition time under 3 minutes with nominal resolution of 1.1 x 1.1 x 2.45 mm. No respiratory triggering or breath-holds were used. The raw data were transferred from the scanner and reconstructed in Matlab (Mathworks, Natick MA), using 2D GRAPPA in k-space and SENSE (R=1) for complex coil combination. The water-fat reconstruction was performed using the method of Berglund et al. (8), as implemented in the ISMRM Fat-Water Toolbox (9). The fat model consisted of 9 peaks plus water at 4.7 ppm, as proposed by Hamilton et al. (10). The reconstructed fat image was shifted in the readout direction to correct for chemical shift, and the signal fat fraction image was calculated as $sFF = \text{fat}/(\text{fat}+\text{water})$. Note that with these parameters there is moderate T1 and T2* weighting that was not corrected, so these sFF measurements give somewhat higher values than an unbiased proton density fat fraction (11). We compared pre-treatment sFF values to values at 6-months by drawing 2D ROIs in representative slices in the L4 vertebral body and the femoral neck, and also in control regions in adipose tissue and skeletal muscle using the Osirix dicom viewer. The Wilcoxon signed-rank test was used to determine significance of the changes in sFF values between baseline and 6-month post treatment for each ROI.

Results: Representative images from chemotherapy and a radiation therapy cases are shown in Figure 1. Both cases show an marked increase in sFF in the lumbar spine and pelvis. The chemotherapy case (Fig 1 a, b) shows changes that are relatively uniform in space, while the radiation therapy case (Fig 1 c, d) shows a large effect within the target radiation field, and decreasing effect further from the pelvis. A time course of the sFF from the L4 vertebral body is shown in Figure 2. There is a general increase of fat fraction detectable at 6 months, with a trend of increased fat fraction at 12 months. Due to population size, statistical tests were only possible at the baseline and 6-month time points. This analysis showed that the sFF increased significantly in both the L4 vertebral marrow (p=0.04) and the femoral necks (p=0.03), while no significant change was observed in control regions.

Discussion: Three dimensional fat fraction imaging was clearly able to show the effect of these cancer therapies on bone marrow composition throughout the pelvic region. The baseline sFF values were notably heterogeneous, and further 3D analyses may help characterize the relationship between pretreatment marrow adiposity on therapy effect. Note that the sFF metric used in this work is biased by both T1 and T2*. These biases can be corrected (12, 13) with modified acquisitions and analysis in future, and this would produce a stronger quantitative metric. While the population size was too small for performing statistical tests at the 12-month time point or for comparing the radiation and chemotherapy groups, the study is ongoing and sized to address these questions in the future.

Conclusion: Water-fat imaging was found to be sensitive to marrow composition changes due to chemotherapy and radiation therapy. This technique could provide a non-invasive biomarker for monitoring bone health during cancer treatment and help guide marrow-related therapeutic interventions such as bone anti-resorptive therapy.

References: 1) Schick F, et al., MRM 1992; 2) Kugel H, et al., JMRI 2001; 3) Yeung DKW, et al., JMRI 2005; 4) Li X, et al., JMRI 2011; 5) Rosen BR, et al., Radiology 1998; 6) Johnson LA, et al., Radiology 1992; 7) Brix G, et al., MRI 1993; 8) Berglund J, et al., MRM 2010; 9) Hu HH, et al., MRM 2012; 10) Hamilton G, et al., NMR Biomed 2011; 11) Reeder SB, et al., JMRI 2011; 12) Liu C-Y, et al., MRM 2007; 13) Yu H, JMRI 2007

Acknowledgements: NIH R03-AR055333, K12-HD055887, and R01-CA154491, PHS Cancer Center Support Grant P30-CA77398, BTRC P41-RR008079 (NCRR) and P41-EB015894 (NIBIB). This work is also supported by our institution's CTSA.

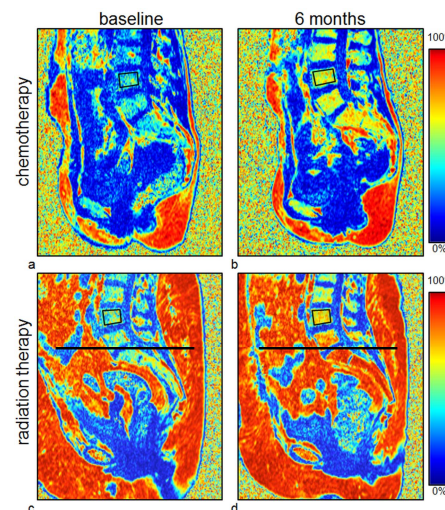


Figure 1 – Sagittal slices from the sFF maps before (a, c) and 6 months after therapy (b, d). The chemotherapy case (a, b) shows uniformly increased sFF throughout the lumbar spine and pelvis, whereas the radiation therapy case (c, d) shows a large increase in the sacral spine, which is within the target radiation field (below black line), compared to the lumbar spine regions outside the target field.

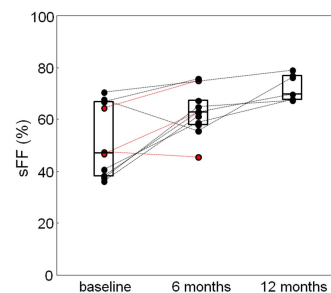


Figure 2 – Time course of the sFF in the L4 lumbar vertebral body (ROIs shown in Fig. 1) over the course of treatment in 11 subjects, shown as individual profile plots overlaid with box plots indicating median and quartile values. Subjects receiving radiation therapy are shown in red; chemotherapy in black.